

Heat Flow Modeling for Controlled Focusing of Microwave Hyperthermia of Breast Cancer: a Computational Feasibility Study

Jaswantsing L. Rajput^{a,*}, Anil B. Nandgaonkar^a, Sanjay L. Nalbalwar^a, Abhay E. Wagh^b

^aDr. Babasaheb Ambedkar Technological University, Lonere, 402103, India.

^bDirectorate of Technical Education, Mumbai, 400001, Maharashtra, India

Corresponding author: *jaswantsing@dbatu.ac.in

Abstract— Heating the tumor tissue with an optimized amount of microwave energy is a promising combinational therapy, called hyperthermia treatment (HT), used with chemotherapy and radiotherapy. This combinational therapy has shown improvement in the survivorship for patients, and life after treatment. In clinical practice, radiation oncologists are still not using HT as a standard therapy because of some side effects like toxicity and hotspots on the surrounding site. To address this issue, optimal focusing of microwave on tumors, with minimal damage of surrounding tissues, is essential to avoid the side effects of HT. Our article briefly discusses on optimal focusing of microwaves on a tumor, computational feasibility study, and analysis of hyperthermia treatment. For the achievement of best outcomes, electrostatic modeling and heat flow modeling of 2D female breast models with tumors have been carried out. The finite element method (FEM) is used to solve the bio-heat equation at the tumor domain, consisting of radiation and convection-based boundary conditions. Obtained simulation results show that the highest focusing of radiation power on and around the tumor inside the breast has been given higher efficiency for hyperthermia. Our 2D modeling simulation results are helpful for improving hyperthermia treatment of breast cancer patients, with minimal damage to cells in the surrounding. Also, the article includes a mathematical analysis of hyperthermia and FEM modeling results concerning temperature distribution, heat flow, electric field intensity, electric flux density, heat flux density, and temperature variations in the breast tumor.

Keywords—Breast cancer; heat flow modeling; hyperthermia treatment (HT); tissue; tumor.

Manuscript received 18 Dec. 2020; revised 15 Apr. 2021; accepted 23 Apr. 2021. Date of publication 31 Aug. 2021.
IJASEIT is licensed under a Creative Commons Attribution-Share Alike 4.0 International License.



I. INTRODUCTION

Breast cancer develops due to the uncontrolled growth of abnormal cells, which evolves as a large mass structure in the breast, called a tumor. Breast cancer alone accounts for 30 % of female cancers. Globally, 1,80,78,957 cancer cases were found in 2018. World Health Organization (WHO) has declared a 1.5% mortality rate of this life-threatening disease. Breast cancer alone caused 5,42,368 deaths of women in 2018 [1]. Worldwide, many researchers are working to find a superior solution for preventing breast cancer, detection at early stages, and better non-invasive treatment to improve patient's quality of life after the treatment and their survivorship. Local hyperthermia is used to raise the temperature of tumor tissue to about 42° C, and simultaneously, the surrounding skin temperature near the tumor region is maintained at about 37 °C.

Numerous clinical trials have proven that it is a promising approach to combine hyperthermia treatment (HT) with

chemotherapy, enhancing certain anticancer drug's effects. The combination of hyperthermia and radiotherapy makes some cancer cells more sensitive to radiation while other normal cells are kept intact [2]-[4]. Tissue characteristics, tumor site, size, temperature control, duration of treatment, and flow of heat in the tumor tissue play a vital role in the effectiveness of HT [3]. Ideally, HT should deposit optimum heat in the tumors without damaging normal tissues. However, normal tissue and tumor tissue have different blood perfusion rates, making complexity for the optimal temperature selection and hence the distribution of heat in the tumor and normal tissues [5], [6].

A higher blood perfusion rate gives a higher cooling effect in the normal tissue [6]. Computerized tomography techniques are generally used to check the proper position of the tumor. Whereas endoscopy, blood tests, and biopsies are used to detect the extent of spreading and the stage of cancer. According to this database, radiation oncologist selects the best suitable treatment for the survival and cure of the cancer patient. Accordingly, a suitable antenna applicator, duration

of treatment on tumor site, and type of hyperthermia application, local or regional, can be decided. Thermometer probes are connected to the tumor and surrounding site to measure and monitor the temperature parameters during the HT [7]. Optical or platinum-type minimally invasive thermometer probes are widely used.

Advanced non-invasive techniques like magnetic resonance imaging (MRI) are widely preferred over invasive ones [8]. Superficial applicators integrated with water boluses apply radiofrequency (RF) energy on the tumor in local hyperthermia. Circulated cold water through boluses helps to avoid overheating of surrounding treatment site and reduction of hotspots. The optimal constrained power focusing (OCPF) based approach is used for solving the complex relationship between electromagnetic waves and thermal focusing [9]. Optimal focusing and shaping of the beam via OCPF based HT planning deliver controlled EM power deposition on tumor tissues while preserving healthy tissues safely. Optimal constrained power focusing provides uniform field distribution at the targeted site with minimum hotspots [10], and multi dipole antenna focusing gives the highest concentration of SAR in the tumor site [11]. Such uniform power distribution and minimum phase angle of focusing create some hotspots on nearby tissues.

Microwave (MW) hyperthermia treatment widely suits breast tumors, and the dielectric properties of breast tumors have a high impact of ultrawideband frequencies [12]. The electrical conductivity of breast tumors is higher, supports the deposition of maximum microwave power focusing on the tumor, and keeps healthy tissue safe. Many experimental simulations are carried out for optimum focusing of MW power on the tumor of the fabricated breast model, which states that 3D focusing of MW power effectively deposits higher radiation for deep-seated tumors [13]-[15]. Groove Gap Waveguide technology with two different frequency applicators can provide optimum focusing of electromagnetic (EM) power in the tumor while delivering low power density in the normal breast tissues [16]. Many researchers and oncologists are collaboratively working to improve the effectiveness and reliability of HT. Recent technological developments have shown promising innovations towards wireless thermal therapy [17]. These developments show that hyperthermia has a bright future in clinical oncology. Adequate RF power focusing on the target site without hotspots is a real challenge in HT. In this article, we propose and analyze this problem in a simulation environment. The goal is to control the heat inside the tumor and reduce hotspots on the surrounding tissues of the tumor site.

II. MATERIALS AND METHODS

A. Research Stages

In this article, the research approach is systematically reported with the following stages.

- The literature study carried out is presented in section I.
- Section II explains the mathematical modeling of heat flow in the tumor, using FEM, and controlled RF focusing with flow chart.
- 2D simulation for target tumor region (breast tumor) explained in section III.

- The understanding from sections I-III has been reported as results and discussion regarding heat flow behavior inside the target tumor region explained in section IV.
- The goal of heat flow modeling has been successfully achieved to control the heat inside the tumor and reduce the hotspots. The article has been concluded briefly in section IV.

B. Basic Arrangement for Hyperthermia of Breast Tumors

Our computational feasibility study is a simulation based on simple 2D geometry of breast model and tumor. The research scope is limited to achieve the controlled focusing of RF, heat flow inside the tumor tissues, and optimum temperature distribution on the target site. We aim to minimize the hotspots in HT. Experimental validation of this methodology will be the scope for future work. The standard working procedure of breast hyperthermia shown in Fig. 1, has been followed to carry out our research in a simulation environment.

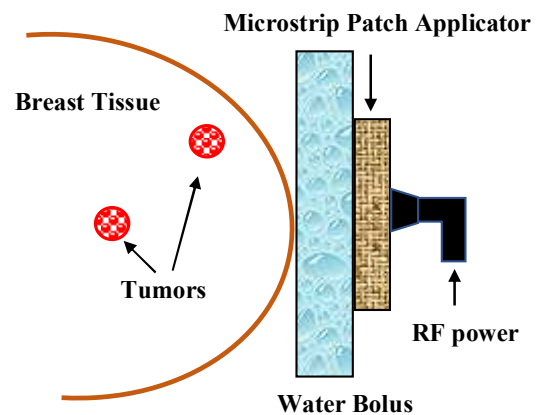


Fig. 1 Arrangement for hyperthermia of breast tumors

Fig. 1 shows a 2D view of a basic arrangement for breast hyperthermia treatment; an RF power source is required to deliver RF energy through a microstrip patch applicator on the tumor site. The cooling bolus is integrated with the antenna system and is coupled at the treatment site to link EM waves properly. Also, it decreases the reflection of EM waves and avoids the loss of EM energy during the HT. According to the temperature rise on the surrounding site, a constant flow of cold water is circulated through the bolus. It controls overheating of the surrounding region of the treatment site. We have used a 2D breast phantom model for simulation in COMSOL Multiphysics solver, V-5.5. The breast model has a radius of 80 mm, and two tumors of 10 mm size are embedded. A finite element-based numerical technique has been used to analyze the heat flow inside the tumors. The hexahedral mesh with 10 elements per wavelength has been used in the solver, generates approximately 0.491 million mesh. The applicator is placed away from the center of the breast model for RF focusing using an excitation frequency of 3.7 GHz.

C. Flow Chart

Fig. 2 depicts the flow chart of the simulation-based computational feasibility analysis for controlled MW focusing on breast cancer hyperthermia. A 2D model of breast phantom with two tumors inside has been used for bio-electromagnetic analysis. Convection and radiation boundary

conditions are used for thermal analysis. The basic settings required for thermal analysis of hyperthermia are as below.

- T_t - Tumor temperature (38~42 °C)
- T_s - Temperature at surrounding tissue (≤ 38 °C)
- $CT1$ -Cooling Temperature for RF ON (15~25 °C)
- $CT2$ - Cooling Temperature for RF OFF (05~15 °C)
- D_t - Duration of HT is properly set (20 min.).

For optimum and iterative MW focusing on tumor site, the alternate direction implicit method [18] is used in the Simulink model. Table I shows electrical properties of human

breast tissue [20], used for modeling at microwave frequency 3.7 GHz, downloaded on October 19, 2020 [19].

TABLE I
ELECTRICAL PROPERTIES OF HUMAN BREAST TISSUE AT 3.7 GHZ

Material	Relative Permittivity	Conductivity [S/m]
Breast Fat	4.8889	0.2408
Muscle	51.1339	2.7814
Skin (dry)	36.7942	2.1788
Coolant-Water Bolus	81.7000	3.1145

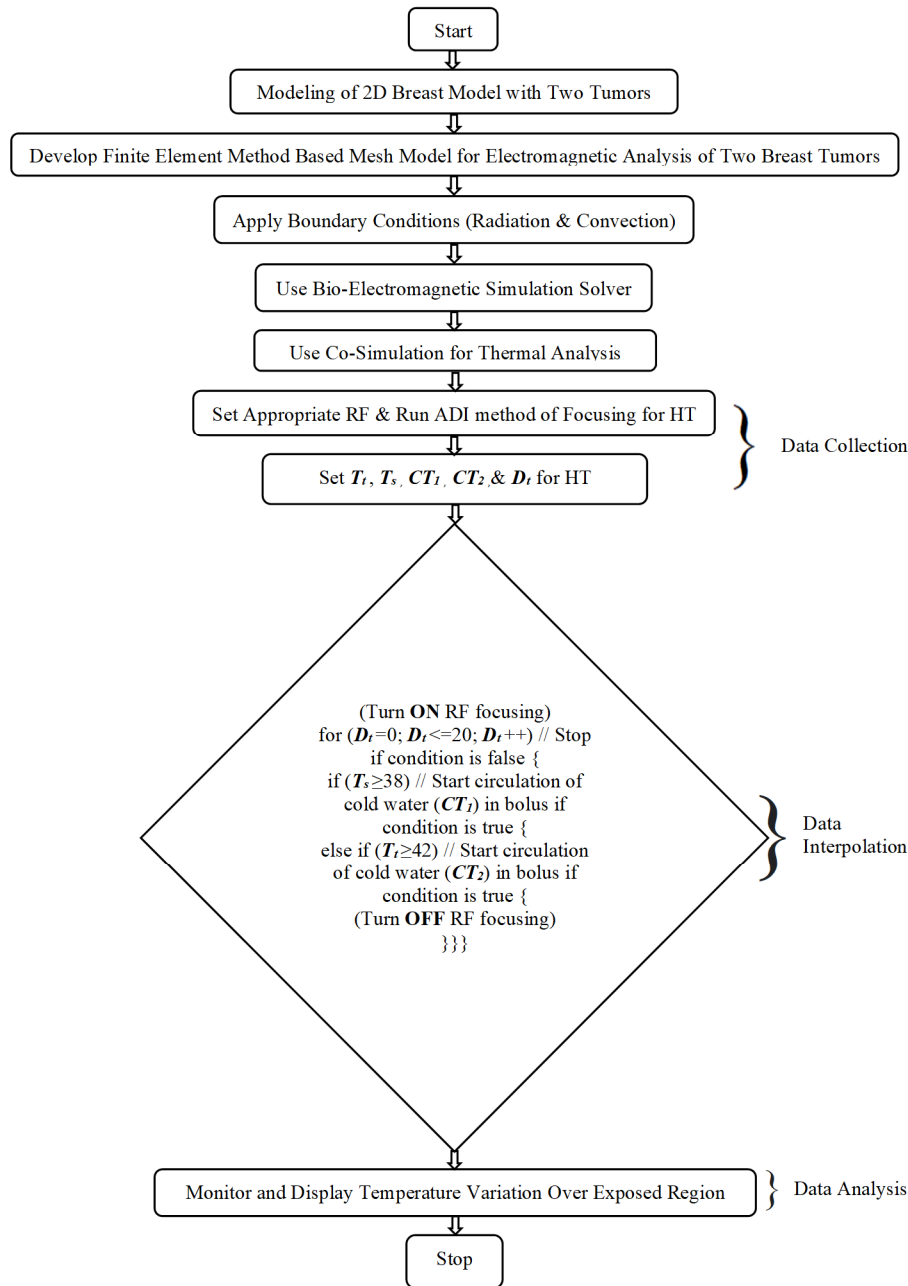


Fig. 2 Flow chart of the computational feasibility study

D. Mathematical Analysis of Hyperthermia

In this section, mathematical analysis of HT is carried out, Pennes bio-heat equation (2) [20] is used for modeling heat flow in the tumor. The heat flow modeling tool has the following different boundary conditions.

- The fixed temperature in kelvin
- Heat flux in W/m²
- Convection (equation-2)
- Radiation (equation-3)
- Periodic
- Anti-Periodic

The flow of heat due to thermal conduction is given in equation (1)

$$f = k \vec{\nabla} T \quad (1)$$

where, f - heat flux vector, k - thermal conductivity coefficient, and $\vec{\nabla} T$ - vector quantity. Equation (2) is the representation of the bio-heat equation for the tumor domain. This equation is solved for radiation and convection boundary conditions using numerical approximation; finite element method (FEM), given in equations (3) and (4), respectively.

$$\rho c \frac{\partial T}{\partial t} = \nabla(k \nabla T) - \omega_b c_b (T - T_b) + Q_m + \alpha P \quad (2)$$

where, ρ - density of the tissue, c - specific heat of breast tissue, k - thermal conductivity of breast tissue, T - temperature, c_b - blood specific heat, ω_b - perfusion rate of blood, T_b - temperature of blood, Q_m - metabolic heat per unit volume, α is the correction parameter that compensates for differences between the velocity of aqueous solution and the intracellular medium, and P - power dissipation per unit volume.

$$k \cdot \frac{\partial T}{\partial n} + h(T - T_0) = 0 \quad (3)$$

$$k \cdot \frac{\partial T}{\partial n} + \beta k_{sb}(T^4 - T_0^4) = 0 \quad (4)$$

where, $\frac{\partial T}{\partial n}$ is the heat emission density in the discrete format used for heat flow modeling, h is the convection heat transfer coefficient, k_{sb} is the Stefan-Boltzmann constant. β is emissivity, T_0 is the surface temperature of the tumor equal to body temperature (37 °C), and T is the variable in terms of heat flow temperature, which varies after exciting the antenna.

A real-time synchronization algorithm is developed with intensive calculations of microstrip patch antenna are merged with electric specifications of human tumor tissues. The breast model, Simulink model, and heat flow modeling are coupled in a simulation environment using COMSOL Multiphysics solver. Fig. 3 shows the Simulink model designed in the simulation environment. The platinum thermometer is used to record the temperature at the tumor site during hyperthermia. We have selected a temperature range of moderate HT (38~42 °C). Feedback control logic is used for monitoring and maintaining the specified temperature on the tumor and surrounding site. The thermometer output is provided to the control logic, and its corresponding temperature has been displayed on a DBATU dashboard. An alternate direction implicit method [18] is used for RF focusing on tumor sites and maintain the appropriate temperature on the tumor site. The transfer function is used to maintain RF focusing and corresponding temperature given by (5).

$$Transfer\ Function = \frac{(HT\ system\ output)}{(Input\ RF\ Power)} \quad (5)$$

Cooling water boluses attached with the antenna applicator also controls the temperature level with the flow of cooling water on the surrounding site. When tumor temperature goes beyond the specified range, highly cooled water (05~15 °C) is circulated through boluses, decreasing the surrounding site's temperature and the tumor site. As soon as tumor temperature

falls below the selected hyperthermia range (38~42 °C), RF focusing will be continued till the duration of hyperthermia treatment (D_t -20 min.). Control logic controls the selected hyperthermia temperature range and focuses on RF on the tumor site, with real-time synchronization.

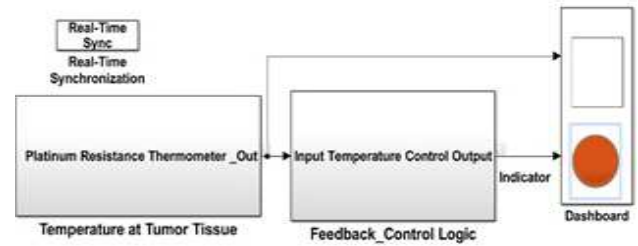


Fig. 3 Simulink model for tumor tissue temperature control system

The coupled simulation of the Simulink model and 2D breast phantom model are used for electrostatic and heat flow modeling of tumors. Simulation results are recorded and presented in section-III.

III. RESULTS AND DISCUSSION

In this simulation-based breast hyperthermia study, we aim to achieve optimum temperature on tumor sites of the breast model. The observations of the controlled tumor temperature are discussed with the obtained results on the Simulink dashboard indicator display, electric flux density, electric field intensity in the tumors, heat flux density in the tumors, and temperature gradient in tumors.

A. Observations of Tumor Temperature Variations on Simulink DBATU Dashboard Indicator Display

Heat flow modeling using radiation and convection boundary conditions is conducted for optimized RF focusing has been described in this section. The modeling computation time is optimized to get better accuracy [18]. The effect of tumor temperature variation on tumor site is observed in electromagnetic solver and continuously visualized in the Simulink DBATU dashboard depicted in Fig. 4.

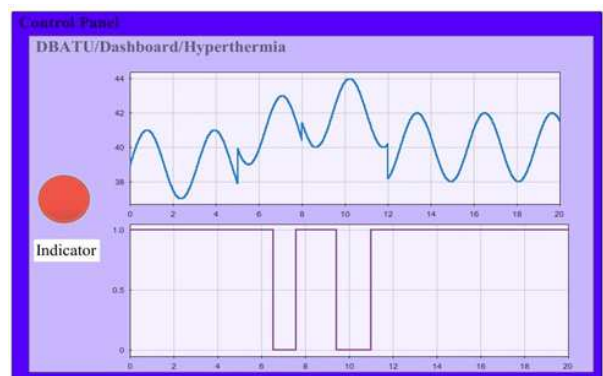


Fig. 4 Simulink DBATU dashboard of the hyperthermia control panel

All temperature variations during the hyperthermia of breast tumor, for 20 minutes, are displayed by the Simulink dashboard indicator shown below. It conveys that our objectives of 2D modeling are accomplished as per the hyperthermia settings in the simulation environment. Table II shows a summary of breast hyperthermia simulation profile, for twenty minutes duration. It shows the working of

Simulink model as per the settings mentioned; tumor temperature ($T_t = 38\text{--}42\text{ }^\circ\text{C}$), and temperature at surrounding tissue ($T_s \leq 38\text{ }^\circ\text{C}$), for the duration of ($D_t = 20\text{ min.}$). All events of simulation model in breast hyperthermia are described with respect to the time duration, RF focusing state, tumor temperature, and required cooling in the Table II.

TABLE II
BREAST HYPERTHERMIA SIMULATION PROFILE SUMMARY

Duration (Minutes. Sec.)	RF State	Tumor Temp. ($^\circ\text{C}$)	Cooling Temp. ($^\circ\text{C}$)	Cooling Time (Min. Sec.)
(0.0~6.30)	ON	(38~42)	(15~25)	(0.0~6.30)
(6.31~7.30)	OFF	(>42)	(05~15)	(6.31~7.30)
(7.31~9.30)	ON	(40~42)	(15~25)	(7.31~9.30)
(9.31~11.0)	OFF	(>42)	(05~15)	(9.31~11.0)
(11.01~20.0)	ON	(40~42)	(15~25)	(11.01~20.0)

The first row indicates the initial phase of simulation; hyperthermia continued up to 6.30 sec with tumor temperature range ($38\text{--}42\text{ }^\circ\text{C}$). As mentioned in the second-row temperature of the tumor site rises above $42\text{ }^\circ\text{C}$, RF focusing, and HT have stopped till the tumor temperature decreases to the selected value $42\text{ }^\circ\text{C}$. Thermal burns due to excessive heating of tumors produce hotspots on nearby tissues. To avoid it, water boluses coupled to the surrounding site provide effective cooling with circulated water ($5\text{--}15\text{ }^\circ\text{C}$). Simulation of breast hyperthermia restarts RF's focusing when tumor site temperature goes below $40\text{ }^\circ\text{C}$, as stated in the third row. Water boluses were used in the Simulink environment for the highest cooling in the range of ($5\text{--}15\text{ }^\circ\text{C}$) to decrease the surrounding tissue and tumor's exceeded temperature during two phases of the simulation, as shown in the second and fourth row. Appropriate RF focusing on tumor site has been achieved by Simulink model indicated in the first, third, and fifth row, with simultaneous cooling at ($15\text{--}25\text{ }^\circ\text{C}$). Additional safety mode is provided to stop the system functioning if any abnormal heating is generated or cooling through the boluses is not achieved.

B. Observations of Electric Field Intensity and Electric Flux Density in Tumors

In the 2D heat flow modeling, the behavior of electric field intensity and electric flux density in the tumor diameter (1 cm) are the important parameters to be observed. The magnitude of electric field density and intensity are also modeled to achieve higher heat flow inside the tumor than the breast's normal cells. Fig. 5 shows the magnitude variation of electric field intensity (V/m) is in the safe range ($0.0005\text{ to }0.003\text{ V/m}$), limits the occurrence of hotspots on nearby sites.

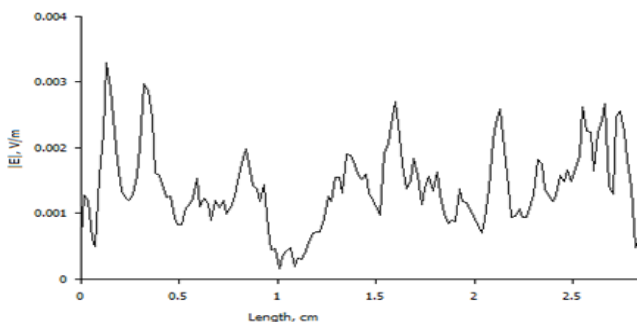


Fig. 5 Electric field intensity around the tumor surface

The magnitude of electric flux density (D) around the tumor surface is shown in Fig. 6. Electric flux density variation around the tumor affects the tumor temperature. Its excessive rise increases the tumor threshold temperature ($\geq 42\text{ }^\circ\text{C}$), which in turn develops hotspots on surrounding healthy tissues. The microstrip patch antenna's primary goal is the controlled electric field distribution, which is observed from the electromagnetic simulation results. Fig. 6 highlights the magnitude variation of electric flux density (Coulombs/m²) over the spread of full circumference of tumor radius 0.5 cm. It shows that electric flux density varies between ($0.5\text{e-}13\text{ to }6.4\text{e-}13\text{ C/m}^2$) on the tumor site.

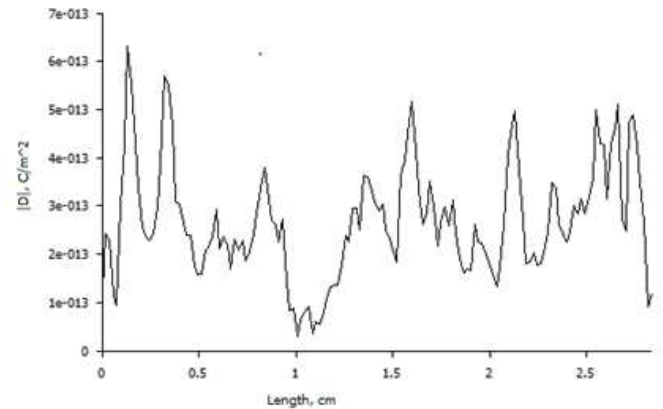


Fig. 6 Magnitude of electric flux density (D) around the tumor surface

C. Observations of Heat Flux Density in Tumors

We achieved maximum RF focusing and in-depth penetration of heat inside the tumors. The main goal to minimize hotspots on nearby sites has also been achieved successfully. The model is one of the best outcomes that showing maximum power distribution in heat flux density (W/m^2) on the tumor site. The computational electromagnetics plot for heat flux density is shown in Fig. 7. The magnitude of heat flux density inside the tumors is maximum, varies in the range of ($22.23\text{--}31.89\text{ W/m}^2$).

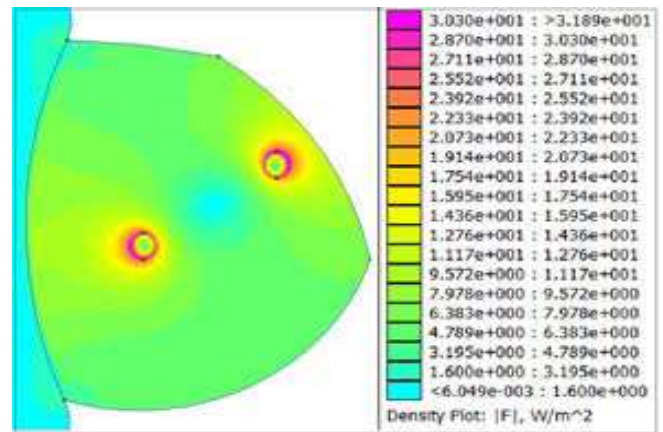


Fig. 7 Heat flux density for breast model

D. Observations of Temperature Distribution in Tumors

It is observed that the temperature distribution around the tumor is higher, whereas it is negligible on normal tissues of the breast. The heat flux density varies from 1 W/m^2 to 31.89 W/m^2 along the line, but it is maximum only at the tumor site.

The temperature gradient distribution around the tumor inside the breast is shown in Fig. 8 with equipotential lines.

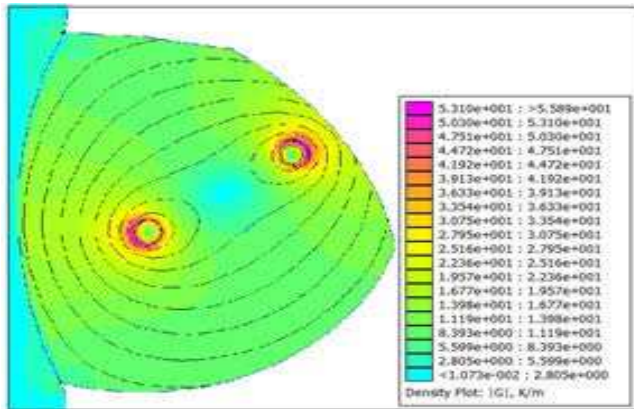


Fig. 8 Temperature gradient with equipotential line

To monitor the temperature distribution inside the breast we have drawn a line that connects these two tumors shown in Fig. 9. It shows the working of breast hyperthermia in the range of (41.35°C ~ 43.75 °C). This temperature range shows the corresponding output of hyperthermia mentioned in the fourth row of simulation profile Table II. The highest concentration of temperature around the tumors and inside the tumors has been achieved in this instance. Such overheating for a long period causes hotspots on the surrounding tissues of the tumors. The control logic plays a vital role in controlling the RF focusing & decreasing the temperature at tumor site lower than 43.75 °C.

The simulated peak value of temperature obtained at the tumor is 43.75 °C, higher than our set value of peak temperature. In the meantime, it is suggested to circulate cold water through the boluses coupled with the tumors and surrounding site to decrease the temperature. HT has been stopped for the treatment duration of (9.31 sec. ~11.0 sec.) to allow cooling of the tumor and surrounding tissues. When cooling decreases the temperature <42 °C, hyperthermia restarted the focusing of RF and heating of tumor sites, shown in the fifth row of Table II. It is continued for the entire treatment duration ($D_t=20$ min.).

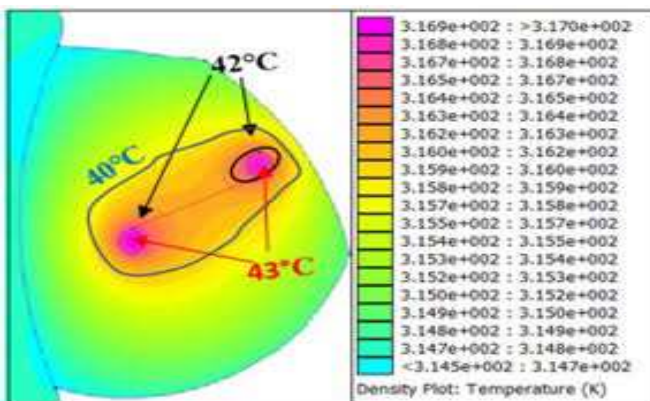


Fig. 9 Cutline between tumors with the highest temperature distribution

The main goal of the modeling has been efficiently achieved, and our simulation-based modeling results indicate that tumor sites are adequately heated in the specified temperature range, with a controlled amount of RF power.

Almost a negligible number of hotspots are observed on the surrounding tissues of the breast tumors.

IV. CONCLUSION

The article discusses heat flow modeling for thermal analysis of breast tumors. Simulation-based electrostatics and heat flow modeling for the breast tumor in the 2D breast phantom has been successfully demonstrated the behavior of heat flux density and electric field intensity distribution inside the breast. Thus, the modeling results show a higher impact of controlled focusing of RF power during the simulation-based hyperthermia of breast cancer. The designed Simulink model has efficiently controlled all parameters of hyperthermia, avoided excessive heat flow, and hence minimized hotspots. An alternate direction implicit method-based focusing approach has been used in this Simulink model for optimum temperature control over the tumor region. Both the tumors in the breast model are heated with controlled focusing of RF, and the results obtained from the modeling are tuned with high accuracy in the simulation platform.

We have carried out this analysis on 2D breast phantom with realistic biological properties at MW frequency of 3.7 GHz. The promising results of our MW focusing methodology need further study on the 3D phantom of the breast model. This study can be further extended for breast hyperthermia with different tumor locations, and the breast's fatty and dense fatty models. Similar studies can be carried out for other types of deadly cancers, like head and neck cancer, where applicator positioning and focusing are a big complexity. The presented simulation results in the article are useful for experimental validation in clinical oncology. Also, future modeling time can be optimized using the fast computing-based system for the analysis of breast tumor hyperthermia.

ACKNOWLEDGMENT

The authors are grateful to Ramrao Adik Institute of Technology, Nerul, Navi Mumbai, for the facilities provided during this research work. We are also thankful to Dr. Nagraj Huilgol, Mumbai, for their constant support and motivation in this research work.

REFERENCES

- [1] IARC Latest Global Cancer Data, Global Cancer Observatory, *IARC, GLOBOCAN Sept-2, 2018*. [Online] Available <https://www.uicc.org/news/new-global-cancer-data-globocan-2018>.
- [2] G. Fiorentini, D. Sarti, C. D. Gadaleta, M. Ballerini, C. Garfagno, T. Ranieri, and S. Guadagni, "A Narrative Review of Regional Hyperthermia: Updates From 2010 to 2019," *Integrative cancer therapies*, vol. 19, pp. 1-13, 2020.
- [3] S. C. Bruning, J. Ijaz, I. Rivens, S. Nill, G. T. Harr, and U. Oelfke, "A comprehensive model for heat-induced radio sensitization," *International Journal of Hyperthermia*, vol. 34, pp. 392-402, 2018.
- [4] Hyperthermia of Breast Cancer: a Computational Feasibility Study N. G. Huilgol, S. Gupta, and C. R. Sridhar, "Hyperthermia with radiation in the treatment of locally advanced head and neck cancer: a report of randomized trial," *Journal of Cancer Research and Therapeutics*, vol. 6, pp. 492-496, 2010.
- [5] J. J. Bosque, G. F. Calvo, V. M. Pérez-García, and M. C. Navarro, "The interplay of blood flow and temperature in regional hyperthermia: a mathematical approach," *Royal Society Open Science*, vol. 8: pp. 1-19, 2021.

- [6] D. Michael, R. Maximilian R, and Christine Allen, "Hyperthermia can alter tumor physiology and improve chemo- and radio-therapy efficacy," *Advanced Drug Delivery Reviews*, vol. 163–164, pp. 98-124, 2020.
- [7] C. P. César, H. RB. Orlande, M. J. Colaço, G. S. Dulikravich, Leonardo, A. B. Varón and B. D. Lamien, "Real-time temperature estimation with enhanced spatial resolution during MR-guided hyperthermia therapy," *Numerical Heat Transfer, Part A: Applications*, vol. 8, pp. 782-806, 2020.
- [8] C. M. V. Leeuwen, A. L. Oei, R. T. Cate, N. A. P. Franken, A. Bel, L. J. A. Stalpers, J. Crezee, and H. P. Kok, "Measurement and analysis of the impact of time-interval, temperature and radiation dose on tumour cell survival and its application in thermoradiotherapy plan evaluation," *International Journal of Hyperthermia*, vol. 34:1, pp. 30-38, 2018.
- [9] D. A. M. Iero, T. Isernia, and L. Crocco, "Thermal and Microwave Constrained Focusing for Patient-Specific Breast Cancer Hyperthermia: A Robustness Assessment," *IEEE Antennas Propagation. Trans.*, vol. 62, pp. 814–821, 2014.
- [10] G. G. Bellizzi, D. A. M. Iero, L. Crocco and T. Isernia, "Three-Dimensional Field Intensity Shaping: The Scalar Case," *IEEE Antennas and Wireless Propagation Letters*, vol. 17, no. 3, pp. 360-363, 2018.
- [11] P. Gas, Miaskowski, and Arkadiusz, "SAR optimization for multi-dipole antenna array with regard to local hyperthermia," *Przegląd Elektrotechniczny*, vol. 95, pp.17-20, 2019.
- [12] M. Lazebnik, *et al.*, "A large-scale study of the ultrawideband microwave dielectric properties of normal, malignant, benign breast tissue obtained from cancer surgeries," *Physics in Medicine & Biology*, vol. 52, no. 20, pp. 6093-6115, 2007.
- [13] L. Xu, and X. Wang, "A Novel Microwave Power Deposition Monitoring Method by Thermoacoustic Imaging," *Cross Strait Quad-Regional Radio Science and Wireless Technology Conference (CSQRWC)*, Xuzhou, 2018, pp. 1-3, 2018. [Online]. Available: <https://doi.org/10.1109/CSQRWC.2018.8455474>.
- [14] P. T. Nguyen, S. Crozier, and A. Abbosh, "Three-Dimensional Microwave Hyperthermia for Breast Cancer in a Realistic Environment Using Particle Swarm Optimization", *IEEE Transactions on Biomedical Engineering*, vol. 64, no. 6, pp. 1335-1344, 2017.
- [15] P. T. Nguyen, A. Abbosh, and S. Crozier, "3-D Focused Microwave Hyperthermia for Breast Cancer Treatment with Experimental Validation," *IEEE Transactions on Antenna & Propagations*. vol.65, no.7, pp.3489-3499, 2017.
- [16] H. F. G. Mendez, M. A. Polochè Arango, F. C. Rico, and I. E. D. Pardo, "Microwave Hyperthermia Study in Breast Cancer Treatment," *Congreso Internacional de Innovación y Tendencias en Ingeniería (CONIITI)*, Bogota, Colombia, 2019, pp. 1-5, 2019. [Online]. Available: <https://doi.org/10.1109/CONIITI48476.2019.8960873>.
- [17] Y. Chen, J. Yi, M. Selvaraj, Y. Hsiang, and K. Takahata, "Wireless Hyperthermia Stent System for Restenosis Treatment and Testing with Swine Model," in *IEEE Transactions on Biomedical Engineering*, vol. 67, no. 4, pp. 2020.
- [18] J. L. Rajput, A. B. Nandgaonkar, S. L. Nalbalwar, and A. E. Wagh, "Design Study and Feasibility of Hyperthermia Technique," in *Computing in Engineering and Technology*, Aurangabad, Maharashtra, India, Jan. 2019, vol. 1025, pp. 721-732, [Online]. Available: <https://doi.org/10.1007/978-981-32, 2020>.
- [19] "Dielectric properties of body tissues," <https://itis.swiss/virtual-population/tissue-properties/database/dielectric-properties, 2020>.
- [20] H. H. Pennes, "Analysis of tissue and arterial blood temperatures in the resting human forearm," *Journal of Applied Physiology.*, vol. 85, pp. 5–34, 1948.